International Journal of Heat and Mass Transfer 77 (2014) 194–201

Contents lists available at ScienceDirect

International Journal of Heat and Mass Transfer

journal homepage: www.elsevier.com/locate/ijhmt

Condensation of R134a outside single horizontal titanium, cupronickel (B10 and B30), stainless steel and copper tubes

Wen-Tao Ji, Chuang-Yao Zhao, Ding-Cai Zhang, Zeng-Yao Li, Ya-Ling He, Wen-Quan Tao *

Key Laboratory of Thermo-Fluid Science and Engineering of MOE, School of Energy and Power Engineering, Xi'an Jiaotong University, Xi'an 710049, People's Republic of China

ARTICLE INFO

Article history:
Received 30 September 2013
Received in revised form 15 April 2014
Accepted 16 April 2014
Available online 5 June 2014

Keywords:
Condensing heat transfer
Refrigerant
Conductivity

ABSTRACT

Experiments were conducted on the condensing heat transfer of eleven horizontal tubes with refrigerant R134a at saturated temperature of 40 °C (1.01 MPa). The tube materials are titanium, cupronickel (B10 and B30), stainless steel and copper, among whom the former four materials are of low thermal conductivity. The enhanced tubes include integral-fin and three dimensional geometries. The results indicate that the heat transfer coefficients of the enhanced copper tube are about 1.6–2.1 times of low thermal conductivity tubes with the same enhanced geometries. Compared with plain tube the mean enhanced ratio of tubes made from titanium, B10, B30 and stainless steel are 8.48, 8.31, 8.22 and 7.52, respectively. The reason why low thermal conductivity affects the condensation heat transfer of enhanced structure is discussed in detail.

1. Introduction

The enhanced heat transfer tubes have been widely used in shell and tube condensers of refrigeration and air-conditioning system. In the past decades, the investigations on condensing heat transfer of vapor outside horizontal tubes could be divided into two aspects: experimental measurements and theoretical predictions. (1) Experimental investigations includes the designing and study of the high performance enhanced geometries [1–5], inundation effects of tube bundles [5–8], and influencing factors in condensing heat transfer [9]. (2) Analytical models [10–12] were also presented for the enhanced tubes, which take following factors into considerations: the distribution of temperature from fin tip to flank, gravity forces and surfaces tensions. It was found that most of the analytical models are only suitable for integral-finned tubes and involve many empirical parameters. Numerical simulation for condensation heat transfer is a multiscale problem in that condensation process is a microscale process and should be simulated by molecular dynamics simulation method while flow in the condensation film is a macroscopic process and can be predicted by macroscale method, say FVM [13]. However, such computer aided direct simulations for condensation process is far from reaching the level of engineering applications. In addition it should be noted that most of the experiments and analytical models were principally conducted for tube materials with high thermal conductivity such as copper.

Even though enhanced tubes of high thermal conductivity, such as copper, are widely used in conventional refrigeration system, there are also some cases where the anticorrosive, anti-impinge, high strength and hardness materials are needed, such as the air-conditioning system where sea water has to be used as the cooling medium. In this case, corrosion prevention is an important factor for the system designing, and special materials have to be adopted which are characterized by low thermal conductivity, such as the cupronickel, titanium and stainless steel. Studies on the vapor condensation on enhanced surface structure made from such metals other than copper are very limited. Following is a brief review on the related references known to the present authors.

Mills et al. [14] experimentally studied the water steam condensation outside horizontal grooved tubes of 19 mm diameter with 36 external fins per inch. Three tube materials were used in the research: copper, brass and cupronickel (70Cu/30Ni). At the downward vapor velocity of 0.6–2.6 m/s, the ratios of heat transfer enhancements over Nusselt analytical solutions for the three materials are respectively of 4.0, 3.6 and 2.6.

Shklover et al. [15] studied the condensing heat transfer of water steam outside one smooth, 3 threaded (41 and 51 fpi) and one rolled (16 fpi) stainless steel tubes, and they found that the finely finned steel tubes did not exhibit much better performance than the smooth tubes. Mitrou [16] experimentally studied the film condensation of water vapor on various threaded tubes made of copper, aluminum, Cu/Ni and stainless steel. It was observed

* Corresponding author. Tel./fax: +86 29 8266 9106.
E-mail address: wqtao@mail.xjtu.edu.cn (W.Q. Tao).

http://dx.doi.org/10.1016/j.ijheatmasstransfer.2014.04.050
0017-9310/

Nomenclature

A	area, m^2
a	slope coefficient in modified Wilson plot method
b	intercept coefficient in modified Wilson plot method
c_i	enhanced ratio of inside heat transfer coefficient
c_p	specific heat capacity, $J \cdot kg^{-1} \cdot K^{-1}$
d	diameter of tube, mm
e	height of outside fin, mm
f	drag coefficient
h	heat transfer coefficients, $W \cdot m^{-2} \cdot K^{-1}$
k	overall heat transfer coefficients, $W \cdot m^{-2} \cdot K^{-1}$
L	tube's tested length, m
m	mass flow rate, $kg \cdot s^{-1}$
n	index of the fitted heat transfer equations
Pr	*Prandtl* number in Gnielinski's correlation
q	heat flux, kW/m^2
r	latent heat of refrigerant, kJ/kg
Re	*Reynolds* number
R_w	thermal resistance of tube wall
t	temperature, °C; height of inside fin, mm

Greek alphabet

ϕ	heat transfer rate, W
λ	thermal conductivity, $W \cdot m^{-1} \cdot K^{-1}$
Δt_m	logrithmic mean temperature difference
μ	viscosity of refrigerant, Pa·s

Subscript

i	inside of tube
in	inlet of tube
ip	inside of plain tube
l	refrigerant liquid
o	outside of tube
out	outlet of tube
p	plain tube
s	saturation
w	wall

that the tube wall thermal conductivity plays an important role in the condensing heat transfer of steam.

The above mentioned researches are concentrated on the condensation heat transfer of water steam, mainly for the power plant condenser applications. Briggs and Rose [17] adopted a semi-empirical model for condensation on horizontal, integral-fin tubes to account for the effect of fin efficiency mainly caused by different thermal conductivity of tube materials. The model agrees satisfactorily with the experimental data of R113 and water steam for typical fin geometries. For R113, the enhancement ratio was found almost independent of the fin thermal conductivity when the conductivities were larger than around 50 $W \cdot m^{-1} \cdot K^{-1}$. They also indicated that the best fin spacing for condensation was only weakly dependent on the fin thermal conductivity. However, the best thickness of the integral fin was more strongly dependent on the fin thermal conductivity.

Zhang et al. [18] studied the condensing heat transfer of R134a and R12 at saturated temperature of 40 °C with low thermal conductivity material of cupronickel. The experimental results of plain tubes agreed well with Nusselt theory within ±10% of R134a and R12. The condensation heat transfer coefficients of R134a are about 32.6% larger than R12 for the cupronickel Thermoexcel-C tube. The average enhanced ratios of the copper Thermoexcel-C tube for R134a and R12 are respectively of 8.08 and 7.20. The cupronickel tube has average enhanced ratio of 3.42 for R134a, and 3.00 for R12 at the same test condition. Their results also show great effect of tube thermal conductivity on condensation heat transfer.

Recently, Fernandez et al. [19–21] studied the condensing heat transfer of different refrigerant outside Cu/Ni and Titanium tubes. They investigated the condensation heat transfer of R22, R417A, R422A and R422D outside Cu/Ni Turbo-C (1575fpm) tube and condensation of R134a and ammonia outside a same Titanium integral-fin (32 fpi) tube. The tubes all have the length of 1895 mm. Experimental results indicate that the condensation heat transfer coefficients of R22 are higher than that of R417A, R422A and R422D outside the Cu/Ni Turbo-C (1575 fpm) tubes in certain degrees. It is also found that the low enhancement ratios are caused by different condensate retention fractions outside the external fins and low thermal conductivity of tube materials. The flooded fractions are different for the same integral-fin tube with different refrigerant. For ammonia the flooded fractions on titanium integral-fin tube are from 62.9% to 73.2%, and the enhanced ratio of condensing heat transfer coefficient ranges from 0.7 to 1.2. While, for R134a, flooded fractions are from 25% to 20% and the enhanced ratio is from 3.09 to 4.1.

The enhanced tube made from these low thermal conductivity materials have strong anti-corrosive character and, to the author's knowledge, recently they become commercially available because of the development of metallurgical and manufacturing technologies. For engineering design purpose more reliable comparison data are needed. In addition, existing literatures are also lack of systematic comparison for condensation heat transfer performance of environmental friendly refrigerant on a series of tubes with low thermal conductivity having the same enhanced structure.

In this paper, the condensing heat transfer of R134a outside 11 tubes made from anti-corrosion materials is studied. The tube materials include Ti, B10-Cu/Ni (90-10), B30-Cu/Ni (70-30), stainless steel and copper. Both plain and mechanically enhanced tubes are studied. Particularly, one copper tube manufactured with the same enhanced geometry as the enhanced B10 tube and another copper tube with the same enhanced geometry as the enhanced stainless steel tube are also studied to investigate the influence of material on the condensing heat transfer.

The rest of the paper is organized as follows. In the second section, experimental apparatus is introduced, including the test loop and the specific structure of the tested enhanced tubes. Then the test procedure is presented in Section 3. Section 4 provides the data reduction method and the measurement uncertainty analysis. The measurement results and discussion are provided in Section 5. Finally some conclusions are summarized in Section 6.

2. Experimental apparatus

The experimental apparatus consists of two cycles: refrigerant circulating system and cooling water circulating system. The schematic diagram of the test apparatus and the two cycles are shown in Fig. 1.

A refrigerant circulation cycle includes the boiler, a condenser, and two ducts connecting the two vessels, which are all made of stainless steel. The condenser has the inner diameter of 147 mm and a length of 1500 mm. The whole apparatus is enwrapped with rubber plastic of thickness 40 mm for insulation; and the rubber plastic is coated with aluminum foil to further prevent the heat loss in the test procedure. In experiment, the refrigerant is heated by an electrical heater, the power of which can be adjusted from 0

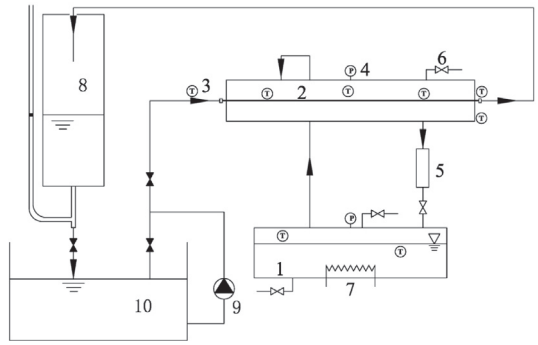

(1)Boiler; (2)Condenser; (3)Thermocouple; (4)Pressure gauge; (5)Condensate measuring container; (6)Exhausting valve; (7)Electric heater; (8)Weight-time flow meter; (9)Water pump; (10)Water storage tank

Fig. 1. Schematic diagram of the experimental apparatus.

to 10 kW. As the liquid refrigerant is heated, it boils, and converts to vapor and rising upward to the condenser. In the condenser, the refrigerant is condensed by the cooling water circulating system that flows through the internal side of tested tube fixed in the condenser, and then the condensed refrigerant returns to the boiler by gravity.

After the cooling water circulates through the tested tube, it flows through a weight–time flow meter to measure the flow rates of cooling water, and then gets back to the water storage tank by a centrifugal pump.

A pressure gauge is used to monitor the pressure of the condenser, and its range is from 0 to 2.5 MPa, which has the precision of ±0.00625 MPa. Five platinum temperature transducers (PT100), with a precision of $\pm(0.15 + 0.002|t|)$ K, are configured in different part of the condenser to measure the vapor and liquid temperatures of the refrigerant. The temperature and temperature difference of water flows through the condenser are measured by a thermal couple and a six-junction copper–constantan thermocouple pile, respectively. The thermocouples and thermocouple pile were calibrated against a temperature calibrator. The calibrator is a mercury thermometer that has the precision of ±0.2 K. Thermocouples are inserted in the central of tube channel and a flow mixer is positioned in front of thermocouples [22]. A Keithley digital voltmeter having the resolution of 0.1 μV is used to measure the electric potential.

The specifications of the test tubes are given in Table 1, where d_o is the diameter of the embryo tube. The test tube name is composed of two parts: before the hyphen is the symbol of tube material, and after the hyphen is the symbol of enhanced structure, where four types of structures are named by C1, C2, C3 and C4, respectively. There are five materials, represented by B10 (Cupronickel), B30 (Cupronickel), Cu (Pure copper), SS (Stainless steel), and Ti (Titanium). The cross section geometries of the enhanced tubes are given in Fig. 2. It worth noting that the cross section dimensions of the same enhanced type but different materials are not strictly identical; it is mainly caused by the different hardness of different material, fluctuation of manufacturing process and different cutting locations for the cross section. The C2, and C3 are three dimensional enhanced tubes, and the C1 and C4 are conventional integral-finned tubes.

3. Experimental procedure

After the tested tubes being fixed in the condenser, the whole system is charged with high pressure nitrogen through the valve fixed in the condenser, nearly 1.2 MPa, 1.2 times of the saturate pressure of R134a at 40 °C. Leakage-check is then performed to ensure the whole system is well sealed at this pressure. This pressure should be kept at least 24 h and if no leakage is detected from the whole system the system seal is satisfied.

Then the system is evacuated to the absolute pressure of at least 800 Pa by a vacuum pump. A small amount of refrigerant is charged into the boiler and then the system is re-evacuated to the absolute pressure of 800 Pa. Repeated this process several times until the content of non-condensable gas is reduced to the acceptable amount. Finally, the refrigerant is charged into the system. In the experiment procedure, the amount of the non condensing gas is checked by two measured saturated temperatures: one measured from the condenser and the other got from the measured pressure in the boiler according to the thermodynamics table. The widely acceptable difference between these two temperatures is 0.2 K [23,24], and this rule of thumb is adopted in the present study. If not, the above charge–discharge process should be repeated to meet this requirement.

For each data run, at least 3 hours are waited for the system to reach a steady state. The steady state in this experiment is characterized by following two indicators: (1) the variation of the required saturation temperature of refrigerant was in the allowed range, usually ±0.05 K of directly monitored result, and (2) the fluctuation of water circulation temperature at inlet of condenser were within ±0.1 K, mostly within ±0.05 K. Then, a group of ten sets of data is recorded for each data-run.

4. Data reduction and uncertainty analysis

The heat (energy) balance is first examined by the output heat transfer rate of cooling water and the electric heating power to determine the accuracy of the experimental measurement system:

The power output from cooling water:

$$\phi_c = m_c c_p (t_{in} - t_{out}) \tag{1}$$

In this equation, t_{in} and t_{out} are respectively the inlet and outlet temperatures of cooling water (K), c_p is the specific heat capacity of cooling water corresponding to the mean temperature of inlet and outlet water (J/kg·K), m_c is the mass flow rate of cooling water (kg/s). The properties of water are taken from [24].

It is required that in the experiment the maximum difference between the two heat transfer rates of cooling and heating should be less than 3%. The average of the two heat transfer rates is used to determine the overall heat transfer coefficients of the tubes. It is written as follows:

$$k = \frac{\phi}{A_o \cdot \Delta t_m} \tag{2}$$

where A_o is the outside surface area determined by the outside diameter of the embryo tube, and Δt_m is the log-mean temperature difference, which is defined as follows:

$$\Delta t_m = \frac{|t_{in} - t_{out}|}{\ln\left(\frac{t_s - t_{in}}{t_s - t_{out}}\right)} \tag{3}$$

where t_s is the saturated temperature of refrigerant vapor.

In this study, the external condensing heat transfer coefficient is separated from the overall thermal resistance:

$$\frac{1}{k} = \frac{A_o}{A_i}\frac{1}{h_i} + R_w + \frac{1}{h_o} \tag{4}$$

In this equation, $R_w = \frac{d_o}{2\lambda_w}\ln\frac{d_o}{d_i}$, the thermal resistance of tube wall. For copper tube this resistance is usually trivial, but for the low thermal conductivity tube it may become appreciable. And the influence of low thermal conductivity tubes is firstly reflected from the thermal resistance of tube wall.

Table 1
Specifications of eleven tested tubes.

Tubes	Outside diameter d_o (mm)	Inside diameter d_i (mm)	Height of outside fin e (mm)	Outside fins per inch	Height of inside fin t (mm)	Length of test section L (mm)	Conductivity of tube material at 293 K ($W \cdot m^{-1} \cdot K^{-1}$) [24,36]
Ti-Plain	19.13	16.19	–	–	–	1500	22
Ti-C1	19.08	15.94	0.422	38	0.234	1500	
B10-Plain	19.00	16.50	–	–	–	1492	61.5
B10-C2	19.15	16.49	0.678	45	–	1500	
B30-Plain	16.00	11.59	–	–	–	1417	28.9
B30-C3	16.01	11.60	0.732	38	–	1411	
SS-Plain	17.92	14.72	–	–	–	1500	15.2
SS-C4	19.00	15.72	0.868	28	–	1487	
Cu-Plain	19.17	16.40	–	–	–	1463	398
Cu-C2	18.92	16.70	0.674	45	–	1470	
Cu-C4	19.09	16.26	0.858	28	–	1449	

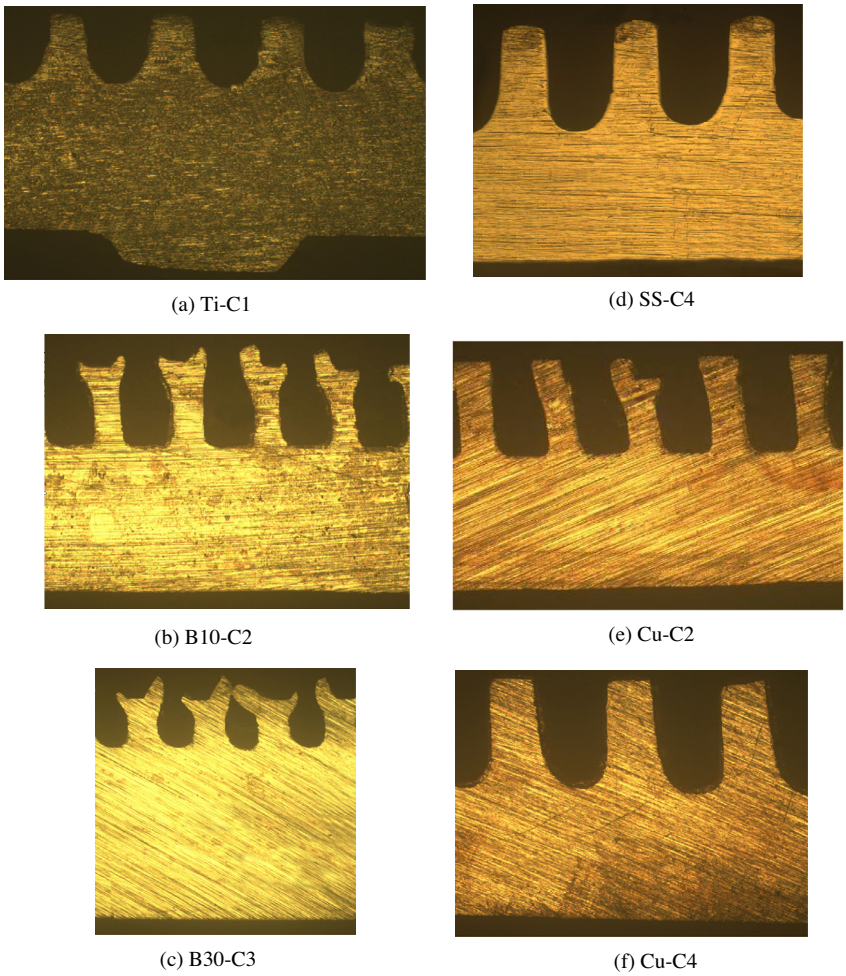

(a) Ti-C1 (d) SS-C4

(b) B10-C2 (e) Cu-C2

(c) B30-C3 (f) Cu-C4

Fig. 2. Geometry of enhanced tubes.

If the inner heat transfer tube is plain, then the h_i can be calculated by Gnielinski equations [25].

$$h_{ip} = \frac{\lambda}{d_i} \frac{(f/8)(\mathrm{Re} - 1000)\mathrm{Pr}}{1 + 12.7(f/8)^{1/2}(\mathrm{Pr}^{2/3} - 1)} \left[1 + \left(\frac{d_i}{L}\right)^{2/3}\right] \left(\frac{\mathrm{Pr}}{\mathrm{Pr}_w}\right)^{0.11} \quad (5)$$

$(\mathrm{Re} = 2300 - 10^6,\ \mathrm{Pr} = 0.6 - 10^5)$

While, if the internal surface of heat transfer tube is enhanced, as tube Ti-C1, then the modified Wilson plot technique is used to obtain the averaged inner water side heat transfer coefficient, h_i. The principles and advantages of the modified Wilson plot technique are presented in Briggs and Yang [26]. For the readers' convenience, the general procedure of this data reduction technique is briefly described as follows.

At a certain velocity variation interval, assuming the inner heat transfer coefficient of the enhanced inner surface is represented by $c_i h_{ip}$, where h_{ip} is the heat transfer coefficient determined by Gnielinski equation at the same fluid velocity and thermal properties for a smooth tube. The experiment is firstly conducted to determine the coefficient c_i, which represents the enhancement ratio of the inner surface structure compared with the internally plain tube. In this experiment, the electric heating power rate and the heat flux

of tube should be kept constant such that h_o is maintained invariant during the test. Then Eq. (4) can be written as:

$$\frac{1}{k} = a\frac{1}{h_{ip}} + b \tag{6}$$

where:

$$a = \frac{d_o}{d_i}\frac{1}{c_i} \tag{7}$$

$$b = \frac{1}{h_o} + R_w \tag{8}$$

By changing the in-tube water flow rate, a group of data is taken and the data are expressed via the equation of a linear straight line shown by Eq. (6). By linear fitting, the slope a and the constant term b can be determined, hence the enhancement ratio of internal heat transfer coefficient c_i is obtained. Fig. 3 shows the Wilson plot for the enhanced tubes Ti-C1 as an example. The reduced c_i of this tube is 1.52.

According to [23,27,28], the measurement uncertainty is now estimated. The confidence level for all measurement uncertainties are assumed to be 95% except indicated individually. The estimated uncertainties of q of the tubes are within 2.4% in the most range of heat transfer rate, and that of k is within 6.3%. h_o is not directly measured, and the uncertainty of h_o is estimated using the method suggested in [24,27]. The uncertainties in h_i is considered of 20% [25]. The estimated uncertainty of h_o for all tubes is within 32.8%. It worth noting that in the recent published well-known heat transfer textbooks [29,30], the prediction error of Gnielinski correlation is regarded as small as 10%. In this paper we estimate it as 20% to be on the safe side.

5. Results and discussion

5.1. Comparison of the overall heat transfer coefficient of eight tubes

Fig. 4 shows the dependence of the overall heat transfer coefficients on the cooling water velocity for the three plain and three enhanced tubes with different materials. Two copper tubes with the same enhanced geometries as tubes B10-C2 and SS-C4 are also presented. The inlet temperature of water for the enhanced tubes and the plain tubes are 35 and 25 °C, respectively. The eight tubes are all without internal enhanced ribs, so at the same water velocity the internal heat transfer coefficients are approximately the same with some minor differences caused by different inner tube diameters and different reference temperatures. This implies that the major differences between the overall heat transfer coefficients are mainly caused by different material thermal conductivity and condensing heat transfer.

As shown in the figure, the eight curves can be grouped into three types: bottom, middle and top. The bottom three tubes are all plain tube without any enhancement of condensation. In the water velocity range tested, the thermal resistance of outside condensation is dominated, hence the overall heat transfer coefficient only show little increase from water velocity of 0.5 to about 4 m/s. For this case the resistance of the low thermal conductivity of the three tubes is not the major part of the total thermal resistance. The overall heat transfer coefficients of the three plain low thermal conductivity tubes are basically all around 1000 W/m^2 K. Carefully inspection of the three curves can find that at the same water velocity the magnitudes of the overall heat transfer coefficients are ranked in the order of B10, B30 and SS, which is caused by the difference of tube thermal conductivity (see Table 1).

The middle two curves show an appreciable effect of water velocity on the overall heat transfer coefficient, indicating that the thermal resistance of the outside condensation heat transfer is comparable to the water side thermal resistance. And the effect of the tube thermal conductivity and outside surface structure can be detected from the difference of the two curves at the same water velocity.

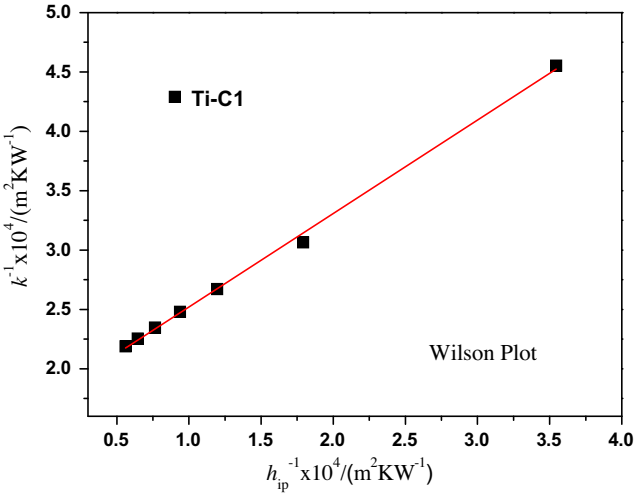

Fig. 3. Wilson plot of tube Ti-C1.

The top three curves show strong effect of the water velocity. For example, the increment in the overall heat transfer coefficient of B10-C2 is 78% from 1.0 to 3.7 m/s, and that of copper tube is about 126%. This simply shows that for the top three tubes the water side thermal resistance is dominated. In addition, the three top curves deviates each other more obvious than the other two groups, because of for this group, the tube thermal resistance becomes more important, and the curve of the copper tube ranks the highest.

5.2. Condensing heat transfer of tubes with different material

In this sub-section the condensation heat transfer coefficient separated from the overall heat transfer coefficients for the tested tubes will be presented and compared. In addition the mechanism why thermal conductivity of tube material does not affect the condensation heat transfer outside plain tubes but does affect condensation on enhanced tubes will be discussed in detail.

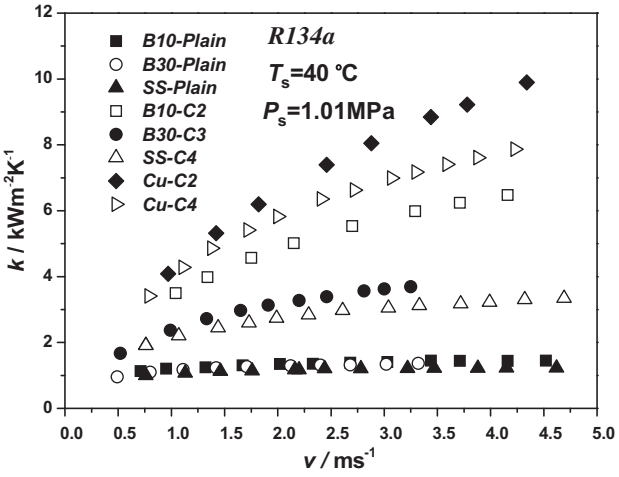

Fig. 4. Overall heat transfer coefficient versus coolant velocity.

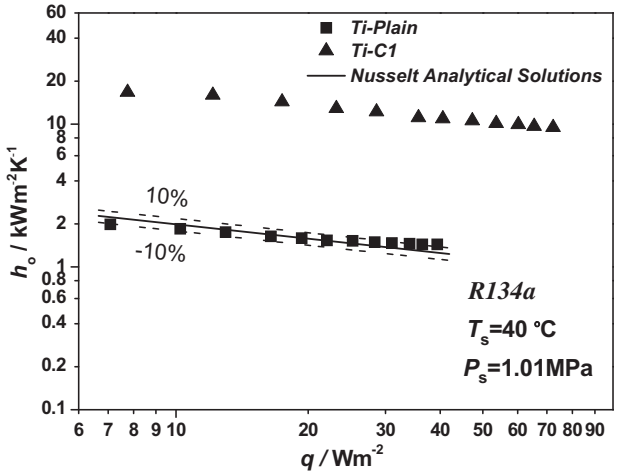

Fig. 5. Condensing heat transfer coefficient versus heat flux of Ti tubes.

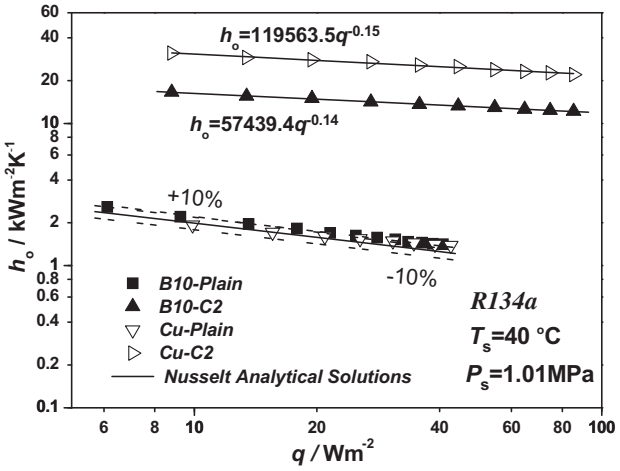

Fig. 6. Condensing heat transfer coefficient versus heat flux of B10 and copper tubes with the same external enhanced geometry.

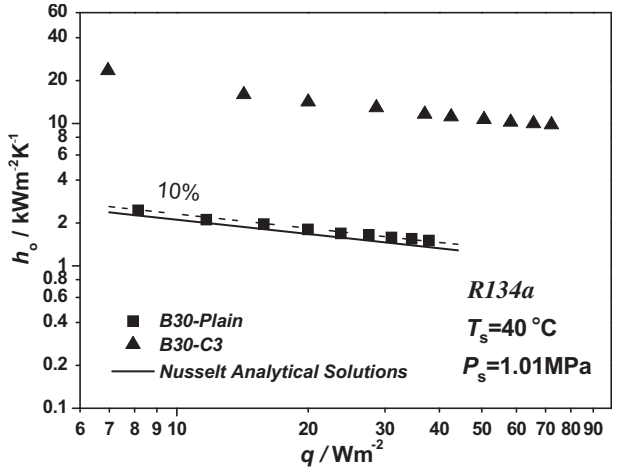

Fig. 7. Condensing heat transfer coefficient versus heat flux of B30 tubes.

First, according to the Nusselt analytical solution of vapor laminar film condensation [31,32], the condensing heat transfer of pure vapor outside horizontal plain tubes is determined by the following equation:

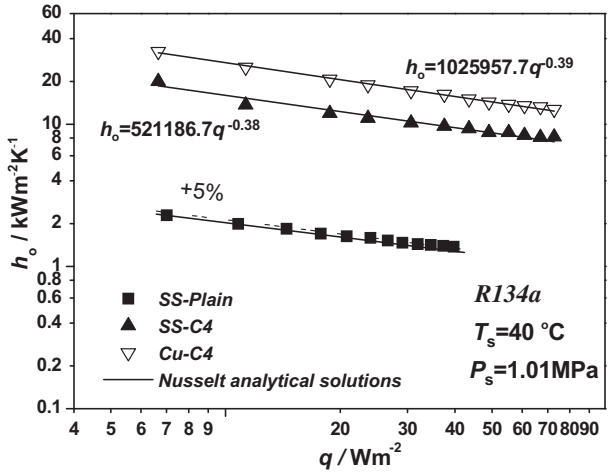

Fig. 8. Condensing heat transfer coefficient versus heat flux of Stainless steel and copper tubes with the same external enhanced geometry.

$$h_p = 0.728\left(\frac{rg\lambda_l^3\rho_l^2}{\mu_l d_o(t_s - t_w)}\right)^{1/4} = 0.656\left(\frac{rg\lambda_l^3\rho_l^2}{\mu_l d_o q}\right)^{1/3} \quad (9)$$

From the above equation, it is observed that the condensing heat transfer outside plain tube is independent of the material. From the physical process of condensation it can be understood as follows. Condensation is driven by the temperature difference between wall and the vapor. For plain or smooth tube, the outside surface is at uniform temperature whether the tube material is of high or low thermal conductivity. Thus for a specified temperature difference or surface heat flux, the condensation heat transfer coefficient can be uniquely determined by Eq. (9). Our experiments for five plain tubes with different thermal conductivity also verify this conclusion. In Figs. 5–8, the lower left part of each figure shows the results for five plain tubes of different materials. It can be seen that all the results agree with Nusselt solution very well. It is to be noted that for the convenience of measurement the heat flux is adopted here as the dependent variable rather than the temperature difference, because for the finned tubes the wall temperature measurement is very difficult.

In order to deepen our understanding of the enhanced tube condensation heat transfer with different thermal conductivity the separated heat transfer coefficients from the overall heat transfer coefficients of the five enhanced tubes are presented in Figs. 5–8 for the C1 to C4, respectively, with heat flux as the abscissa. From the figures following features may be noted.

First, a general feature can be found that the separated condensation heat transfer coefficients of all the enhanced tubes decrease with the increase in heat flux, that is, decrease with the increase in temperature difference. In term of $h \propto q^n$ the values for different tubes are as follows:

$$\begin{array}{ll} \text{Ti-C1} & n = -0.27 \\ \text{B10-C2} & n = -0.14 \\ \text{Cu-C2} & n = -0.15 \\ \text{B30-C3} & n = -0.39 \\ \text{Cu-C4} & n = -0.39 \\ \text{SS-C4} & n = -0.38 \end{array} \quad (10)$$

Second, from Figs. 5 and 7 it can be seen that the enhanced Ti-C1 and B30-C3 tube can significantly enhance condensation heat transfer. Compared with plain tubes of the same material, in the test heat flux range, the average enhanced ratios are respectively of 8.48, 8.31, 8.22 and 7.52 for Ti-C1, B10-C2, B30-C3 and SS-C4.

Third, from Figs. 6 and 8 it is obvious that for the enhanced structure tubes thermal conductivity has appreciable effect on the separated condensation heat transfer coefficients. For the enhanced geometry of C2, the heat transfer coefficients of copper tube are 1.8–2.1 times greater than the B10 tube (Fig. 6), and it is 1.6 to 1.8 times of Cu over the stainless steel tubes for the enhanced geometry of C4 (Fig. 8).

Now attention is turned to the analysis why tube thermal conductivity affects the condensing heat transfer of the enhanced structure. It is generally recognized that the effect is caused by the fin efficiency [17,19,33]. Yet detailed analysis has to be performed in order to get convinced explanation. As shown in Eq. (10) and Figs. 5–8 for the enhanced tubes the condensation heat transfer coefficient decreases with the increase in heat flux, that is, decreases with the increase in temperature difference, $t_s - t_w$, where t_s, t_w are saturated and wall temperature respectively. For the simplicity of qualitative discussion, it may assume that for the enhanced structure $h \propto \Delta t^{-0.25}$. Suppose for two enhanced tubes with the same structure but different thermal conductivity, the root wall temperatures are the same (below the vapor saturated temperature), according to the fin conduction analysis [24,34], the fin temperature of the low thermal conductivity will be higher than that of the higher thermal conductivity, implying that the temperature difference ($t_s - t_w$) of the low thermal conductivity tube is smaller than that of the higher thermal conductivity. In this sense the fin local heat transfer coefficient of the low thermal conductivity tube would be higher. However, the local heat transfer rate is the production of heat transfer coefficient and the temperature difference, that is, $q = h\Delta t \propto \Delta t^{3/4}$. The local fin temperature difference (i.e., the difference between saturated temperature and local fin temperature) of the low thermal conductivity tube is less than that of the higher thermal conductivity tube, so is the fin heat flux. Hence the total heat transfer rate of the higher thermal conductivity tube will be larger than that of the low thermal conductivity tube. If we write the Newton's law of cooling for the condensation side, we have: $Q_{o,tot} = A_{o,eff} h_o \Delta t$. Here for the two tubes with different material, the temperature difference is the same (saturated temperature minus root tube wall temperature), the effective heat transfer area of the low thermal conductivity tube will be a bit smaller than that of the higher thermal conductivity tube because of low fin efficiency, while the total heat transfer rate of the low thermal conductivity tube will be more appreciably less than that of the higher thermal conductivity tube, making its averaged heat transfer coefficient being lower than that of the higher thermal conductivity tube.

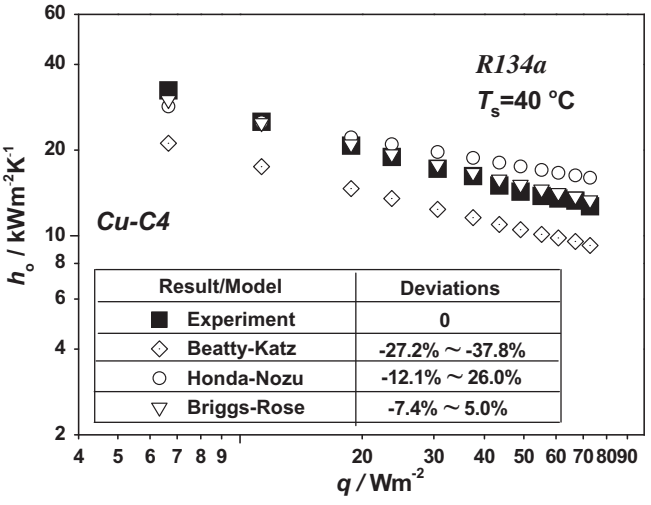

Fig. 9. Comparisons of experiment result and three prediction models for tube Cu-C4.

Fig. 9 compares the experimental condensation heat transfer coefficient with that predicted by theoretical models, including the models of Beatty–Katz [35], Honda [10] and Briggs–Rose [17], for the integral-fin tube Cu-C4. It is found that Honda and Briggs–Rose models can predict the experimental results within a range of ±26%. However, the deviations of Briggs–Rose and Honda model to predict the stainless steel tube SS-C4 are generally in the range of ±50–70%. Beatty–Katz model can predict the stainless integral tube SS-C4 accurately in the range of −0.7% to 11.2%.

6. Conclusions

The R134a condensing heat transfer of eight horizontal tubes with enhanced surface structure and made from four low thermal conductivity materials is experimentally studied in this paper. The four materials are titanium, cupronickel (B10 and B30), stainless steel. For comparison purpose one plain and two enhanced copper tubes with the same fin geometries as B10 and stainless steel tubes are also tested. Two types of enhanced structures are investigated, integrated low-fin and three-dimensional fin. The overall heat transfer coefficients are measured with inner water velocity ranging from 0.5 to 4 m/s. Thermal resistance separation method is adopted to obtain the condensation side heat transfer coefficients. Detailed discussion is presented to analyze why the tube thermal conductivity affects the condensation heat transfer of enhanced tubes. The major findings are as follows:

(1) For the same enhanced structure the tube made from higher thermal conductivity has appreciably higher condensation heat transfer coefficient than that of low thermal conductivity tube. Within the tested range, the condensation heat transfer coefficients of copper tube may be 1.6–2.1 times of those with low thermal conductivity.
(2) Compared with plain tube, the enhanced structure studied made from low thermal conductivity materials can significantly enhance condensation heat transfer, and within the range tested an enhanced ratio up to eight may be reached.
(3) The separated condensation heat transfer coefficients of the enhanced structure made from low thermal conductivity materials decrease with the increase in surface heat flux. In terms of $h \propto q^n$, the exponent n varies from −0.14 to −0.39.
(4) The lower fin efficiency resulted from low material thermal conductivity is the major reason that condensation heat transfer coefficient of tubes with low thermal conductivity is inferior to that of higher thermal conductivity.

Acknowledgments

This work was supported by the National Key Fundamental Research Projects (973) (2013CB228300) and Specialized Research Fund for the Doctoral Program of Higher Education (SRFDP) (No. 20130201120057).

References

[1] R. Kumar, A. Gupta, S. Vishvakarma, Condensation of R-134a vapour over single horizontal integral-fin tubes: effect of fin height, Int. J. Refrig. 28 (3) (2005) 428–435.
[2] K.-J. Park, D.G. Kang, D. Jung, Condensation heat transfer coefficients of R1234yf on plain, low fin, and Turbo-C tubes, Int. J. Refrig. 34 (1) (2011) 317–321.
[3] M. Christians, M. Habert, J.R. Thome, Film condensation of R-134a and R-236fa, part 1: experimental results and predictive correlation for single-row condensation on enhanced tubes, Heat Transfer Eng. 31 (10) (2010) 799–808.

[4] Z. Zhang, Q. Li, T. Xu, X. Fang, X. Gao, Condensation heat transfer characteristics of zeotropic refrigerant mixture R407C on single, three-row petal-shaped finned tubes and helically baffled condenser, Appl. Therm. Eng. 39 (2012) 63–69.
[5] T. Gebauer, A.R. Al-Badri, A. Gotterbarm, J.E. Hajal, A. Leipertz, A.P. Fröba, Condensation heat transfer on single horizontal smooth and finned tubes and tube bundles for R134a and propane, Int. J. Heat Mass Transfer 56 (1) (2013) 516–524.
[6] D. Gstoehl, J.R. Thome, Film condensation of R-134a on tube arrays with plain and enhanced surfaces: part II – empirical prediction of inundation effects, ASME J. Heat Transfer 128 (1) (2006) 33–43.
[7] D. Gstoehl, J.R. Thome, Film condensation of R-134a on tube arrays with plain and enhanced surfaces: part I – experimental heat transfer coefficients, ASME J. HeatTransfer 128 (1) (2006) 21–32.
[8] W.-T. Ji, C.-Y. Zhao, D.-C. Zhang, Y.-L. He, W.-Q. Tao, Influence of condensate inundation on heat transfer of R134a condensing on three dimensional enhanced tubes and integral-fin tubes with high fin density, Appl. Therm. Eng. 38 (2012) 151–159.
[9] C.L. Fitzgerald, A. Briggs, J.W. Rose, H.S. Wang, Effect of vapour velocity on condensate retention between fins during condensation on low-finned tubes, Int. J. Heat Mass Transfer 55 (4) (2012) 1412–1418.
[10] H. Honda, S. Nozu, A prediction method for heat transfer during film condensation on horizontal low integral-fin tubes, ASME J. Heat Transfer 109 (1) (1987) 218–225.
[11] A. Briggs, J.W. Rose, Evaluation of models for condensation heat transfer on low-finned tubes, J. Enhanc. Heat Transfer 6 (1) (1999) 51–60.
[12] A.R. Al-Badri, T. Gebauer, A. Leipertz, A.P. Fröba, Element by element prediction model of condensation heat transfer on a horizontal integral finned tube, Int. J. Heat Mass Transfer 62 (2013) 463–472.
[13] Y.L. He, W.Q. Tao, Multiscale simulations of heat transfer and fluid flow problems, ASME J. Heat Transfer 134 (2010) 031018-1–13.
[14] A.F. Mills, G.L. Hubbard, R.K. James, C. Tan, Experimental study of film condensation on horizontal grooved tubes, Desalination 16 (2) (1975) 121–133.
[15] G.G. Shklover, O.O. Mil'man, V.S. Baskov, G.A. Ankudinov, Heat transfer in condensation of steam on finely-finned horizontal tubes, Heat Transfer – Sov. Res. 13 (2) (1981) 108–114.
[16] E. Mitrou, Film Condensation Heat Transfer on Horizontal Finned Tubes, Naval Postgraduate School, Monterey, CA, 1986.
[17] A. Briggs, J.W. Rose, Effect of fin efficiency on a model for condensation heat transfer on a horizontal, integral-fin tube, Int. J. Heat Mass Transfer 37 (Supplement 1) (1994) 457–463.
[18] D.C. Zhang, W.T. Ji, W.Q. Tao, Condensation heat transfer of HFC134a on horizontal low thermal conductivity tubes, Int. Commun. Heat Mass Transfer 34 (8) (2007) 917–923.
[19] J. Fernandez-Seara, F.J. Uhia, R. Diz, Experimental analysis of ammonia condensation on smooth and integral-fin titanium tubes, Int. J. Refrig. 32 (6) (2009) 1140–1148.
[20] J. Fernández-Seara, F.J. Uhía, R. Diz, A. Dopazo, Condensation of r-134a on horizontal integral-fin titanium tubes, Appl. Therm. Eng. 30 (4) (2010) 295–301.
[21] J. Fernandez Seara, F.J. Uhia, R. Diz, J.A. Dopazo, Vapour condensation of R22 retrofit substitutes R417A, R422A and R422D on CuNi turbo C tubes, Int. J. Refrig. 33 (1) (2010) 148–157.
[22] J.W. Rose, Heat-transfer coefficients, Wilson plots and accuracy of thermal measurements, Exp. Therm. Fluid Sci. 28 (2–3) (2004) 77–86.
[23] B. Cheng, W.Q. Tao, Experimental study of R-152a film condensation on single horizontal smooth tube and enhanced tubes, ASME J. HeatTransfer 116 (1) (1994) 266–270.
[24] S.M. Yang, W.Q. Tao, Heat Transfer, Higher Education Press, Beijing, 2006.
[25] V. Gnielinski, New equations for heat and mass transfer in turbulent pipe and channel flows, Int. Chem. Eng. 16 (1976) 359–368.
[26] D.E. Briggs, E.H. Young, Modified Wilson plot techniques for obtaining heat transfer correlations for shell and tube heat exchangers, Chem. Eng. Prog. Symp. Ser. 92 (65) (1969) 35–45.
[27] S.J. Kline, F.A. Mcclintock, Describing uncertainties in single-sample experiments, Mech. Eng. 75 (7) (1953) 3–9.
[28] W.T. Ji, D.C. Zhang, N. Feng, J.F. Guo, M. Numata, G.N. Xi, W.Q. Tao, Nucleate pool boiling heat transfer of R134a and R134a-PVE lubricant mixtures on smooth and five enhanced tubes, ASME J. Heat Transfer 132 (11) (2010) 11502.
[29] YunusA Cengel, AfshinJ Ghajar, Heat and Mass Transfer, fourth ed., Springer, Berlin, 2011.
[30] Theodore L. Bergman, Adrinne S. Lavine, Frank P. Incropera, David P. DeWitt, Introduction to Heat Transfer, sixth ed., John Wiley & Sons, Inc., Hoboken, NJ, 2011.
[31] W. Nusselt, Die oberflachencondensation des wasserdampfes, VDI 60 (1916) 541–569.
[32] V. Dhir, J. Lienhard, Laminar film condensation on plane and axisymmetric bodies in nonuniform gravity, ASME J. Heat Transfer 93 (1971) 97.
[33] L. Burmeister, Vertical fin efficiency with film condensation, ASME J. Heat Transfer 104 (1982) 391.
[34] Y.A. Cengel, Heat Transfer: A Practical Approach, second ed., McGraw-Hill, Boston, 2003.
[35] K.O. Beatty, D.L. Katz, Condensation of vapors on outside of finned tubes, Chem. Eng. Prog. 44 (1) (1948) 908–914.
[36] Y.S. Touloukian, R.W. Powell, C.Y. Cho, P.G. Klemens, Thermal Conductivity: Metallic Elements and Alloys, Plenum Press, New York, 1970.